

Lateral Flow Test (LFT) Detects Cell-Free MicroRNAs Predictive of Preterm Birth Directly from Human Plasma

Loukia Petrou, Elmeri Latvanen, Florent Seichepine, Sung Hye Kim, Phillip R. Bennett, Lynne Sykes, David A. MacIntyre, Vasso Terzidou,* and Sylvain Ladame*

Despite extensive research toward the development of point-of-care nucleic acid tests (POC NATs) for the detection of microRNAs (miRs) from liquid biopsies, major hurdles remain including the strict requirement for extensive off-chip sample preprocessing. Herein, a nucleic acid lateral flow test (NALFT) is reported on that enables the direct detection of endogenous miRs from as little as 3 μ L of plasma without the requirement for any enzyme-catalyzed target amplification or complex miR extraction steps. This is achieved through integration of a denaturing hydrogel composite material onto the LFT, allowing for near-instantaneous on-chip release of miRs from their carriers (extracellular vesicles or transport proteins) prior to detection. This next-generation LFT is sensitive enough to detect endogenous concentrations of miR-150-5p, a predictive biomarker for preterm birth (PTB) found deregulated in maternal blood from as early as 12th week of pregnancy. Herein, a key step is represented toward a first bedside test for risk-stratification during pregnancy by predicting true outcome at a very early stage. More generally, the universal and versatile nature of this novel sample preprocessing platform can further improve the robustness of existing NALFTs and facilitate their application at the POC.

born preterm, resulting in 1 million deaths per year.^[1,3] Out of the surviving infants, those born before 28 weeks of gestation are especially at increased risk of neurodevelopmental disorders and chronic health conditions.^[4,5] Screening tools available include cervical length measurement and fetal fibronectin but are only recommended for high risk of PTB pregnancies defined as either those with a previous PTB, mid-trimester loss, or cervical trauma and are not suitable for population-wide risk stratification.^[6] They are both costly and more importantly can only predict imminent birth, narrowing the window for intervention.^[6] Moreover, although 25% of PTBs are planned due to preexisting health conditions such as pre-eclampsia or extreme growth restriction, 50% of all PTBs happen in women with no previously identifiable risk factors, many of who are in their first pregnancy.^[7] This highlights the need for a screening tool that would enable closer monitoring and follow-up of all pregnant women at high risk of PTB early on,

ideally taken as part of the first few antenatal appointments (between the 10th and 14th week) alongside screening tests for Down syndrome, Edwards' syndrome, and Patau's syndrome.


MicroRNAs (miRs) are short, noncoding RNAs that have recently emerged as promising biomarkers for a wide array of diseases. They are involved in posttranscriptional gene regulation in a

1. Introduction

Preterm birth (PTB) is the birth before the 37th week of pregnancy and is currently the leading cause of death in children under 5.^[1,2] Recent advancements in medicine and biotechnology have improved infant survival rates substantially; however, about 1 in 10 babies are

L. Petrou, E. Latvanen, F. Seichepine, S. Ladame
Department of Bioengineering
Imperial College London
W12 0BZ London, UK
E-mail: sladame@imperial.ac.uk

S. H. Kim, P. R. Bennett, L. Sykes, D. A. MacIntyre, V. Terzidou
March of Dimes European Preterm Birth Research Centre
Imperial College London
W12 0NN London, UK
E-mail: v.terzidou@imperial.ac.uk

 The ORCID identification number(s) for the author(s) of this article can be found under <https://doi.org/10.1002/anbr.202200026>.

© 2022 The Authors. Advanced NanoBiomed Research published by Wiley-VCH GmbH. This is an open access article under the terms of the Creative Commons Attribution License, which permits use, distribution and reproduction in any medium, provided the original work is properly cited.

DOI: 10.1002/anbr.202200026

S. H. Kim, P. R. Bennett, L. Sykes, D. A. MacIntyre, V. Terzidou
Institute of Reproductive and Developmental Biology
Imperial College London
W12 0NN London, UK

P. R. Bennett
Queen Charlotte's and Chelsea Hospital
Imperial College NHS Trust
W12 0HS London, UK

L. Sykes
The Parasol Foundation Centre for Women's Health and Cancer Research
St Mary's Hospital
Imperial College NHS Trust
W2 1NY London, UK

P. R. Bennett, V. Terzidou
Department of Obstetrics & Gynaecology
Chelsea and Westminster Hospital NHS Trust
SW10 9NH London, UK

variety of proposed ways including ribosome stalling, mRNA degradation, and competing for mRNA cap binding to name a few.^[8–10] Their involvement in these natural regulatory mechanisms means that in pathophysiological states, they are often dysregulated in ways that either bring about the disease or are resulting from it due to the pathological changes taking place, as demonstrated previously in the case of cancer.^[11–13] Different expression profiles of deregulated miRs have been identified that are characteristic of specific diseases. These can be exploited not only for their diagnostic and prognostic value but also as predictive biomarkers, as recently demonstrated for PTB. In a high-risk population, miR-150-5p emerged as the most promising single blood biomarker for PTB prediction (area under the receiver operator characteristic curve [AUC] = 0.87), from as early as the 12th week of pregnancy. This resulted in a sixfold increase in miR-150-5p levels in women who delivered preterm and 4.5-fold increase in women with early cervical shortening compared to levels observed in women who ended up delivering at term with no early cervical shortening, in the 12–14⁺⁶ time frame.^[14] Interestingly, miR-150-5p upregulation naturally occurs throughout pregnancy in term births with an overall sixfold increase between the 1st and the 3rd trimester.^[15] The role of miR-150-5p has been linked to the NFκB pathway which is the inflammatory pathway linked to initiation of parturition.^[16,17] Abnormal early upregulation of miR-150-5p in maternal blood during the first trimester thus can be used as a reliable predictive indicator for PTB proving its promising potential for the development of a minimally invasive bedside screening test.

Despite the proven potential of miRs as clinically useful biomarkers, no miR-sensing device has yet been able to bridge the translational gap and make its way into clinical practice. This is in large part due to the inability of most miR-sensing technologies to detect such biomarkers directly from bodily fluids and their reliance on efficient and consistent sample processing and biomarker extraction prior to detection. Most commonly being found within extracellular vesicles (such as exosomes), or associated to proteins (e.g., Argonaute 2) or protein complexes,^[18] miRs are very stable in biological fluids and remain stable after multiple freeze-thaw cycles, pH and temperature changes, and extensive storage.^[19] They are however mostly inaccessible and undetectable by traditional miR-sensing probes when under this form, requiring the need for total miR extraction prior to any detection. Such extraction steps are typically complex and not easily amenable to incorporation into POC test. By controlling the number of miRs released from their cargo and available for detection, these processing steps are a major source of variability and error, which have resulted in major inconsistencies in the literature. Although miR-150-5p was reported to be preferentially found in extracellular vesicles,^[20,21] Arroyo et al. and Turchinovich et al. demonstrated that cell-free miRs are mainly transported by Argonaute 2 when circulating in serum, plasma, and cell culture media.^[22,23] However, this was directly contradicted by other work showing that miRs in saliva and serum are mainly within exosomes,^[24] highlighting not only the intricacy of the field but also the inconsistency in the literature due to the lack of standardized protocols for miR extraction and detection.^[25]

Recently developed miR-sensing strategies enabled the detection of endogenous concentrations of these circulating biomarkers without the need for any enzyme-catalyzed target amplification

steps, preventing errors associated with amplification biases. This includes single-molecule detection nanotechnologies which, despite ultrahigh sensitivity, often require expensive equipment not easily amenable to miniaturization.^[26] Other molecular probes have also been developed and preclinically validated that are more amenable to incorporation into point-of-care (POC) devices. Peptide nucleic acid (PNA) probes in particular were successfully engineered that could detect miRs quantitatively through oligonucleotide-templated reaction (OTR).^[27] Early attempts to implement this molecular-sensing strategy onto lateral flow assays (LFAs) showed great promise in terms of sequence specificity (down to single nucleotide) and sensitivity (amplification-free detection of endogenous miRs extracted from blood).^[28] However, these studies, like many others, fell short of being able to detect circulating miRs directly from unprocessed blood plasma or serum, preventing the development of a full POC test.

Lateral flow tests (LFTs) allow for rapid, cheap sensing for diagnostic, prognostic, and screening strategies with a long shelf life and small sample volume requirements making them an ideal POC-sensing tool.^[29] Notable examples include the pregnancy test and more recently the antigen test for COVID-19. In the case of COVID-19 the low cost and ability of rapid diagnosis has turned LFTs into an invaluable and accessible tool in the global effort to control the disease and highlights their usefulness at scale. The ideal LFT should be affordable, require minimal or no sample preprocessing and provide an easily accessible readout to allow for translation to the POC. Herein, we present the first example of LFT with automated on-chip sample processing for semiquantitative miRNA detection directly from human plasma (**Figure 1**). Within this proof-of-concept study, LFTs were shown to detect endogenous levels of miR150-5p from only 3 μL of plasma in as little as 45 min and were able to distinguish between patients at low and high risk of PTB with $p < 0.0001$.

2. Results

First implementations of OTRs onto LFTs for miRNA sensing have recently been described by Pavagada et al., Sayers et al., and Farrera-Soler et al.^[28,30,31] Despite reporting good levels of sensitivity and sequence specificity, these initial attempts all required a significant amount of off-chip pre- and/or post-processing precluding their potential application as a clinically useful POC or bedside test. Most notably, these LFTs could only be used on pre-purified miR extracts, necessitating the cumbersome and error-prone miR extraction to be performed in solution prior to the test. In the absence of standardized protocol, this preprocessing is a commonly accepted source of error and variation between studies and remains one of the main bottlenecks in the development of POC tests based on miR detection.^[25,32–34] Herein, we are reporting on the design and preclinical validation of a versatile and easily tuneable LFT for the amplification-free detection of miR-150-5p, a predictive biomarker for PTB, directly from human plasma.

2.1. LFT Manufacturing and In Vitro Testing

On-chip miR detection was achieved using a fluorogenic OTR between two bespoke PNA probes modified with a quenched

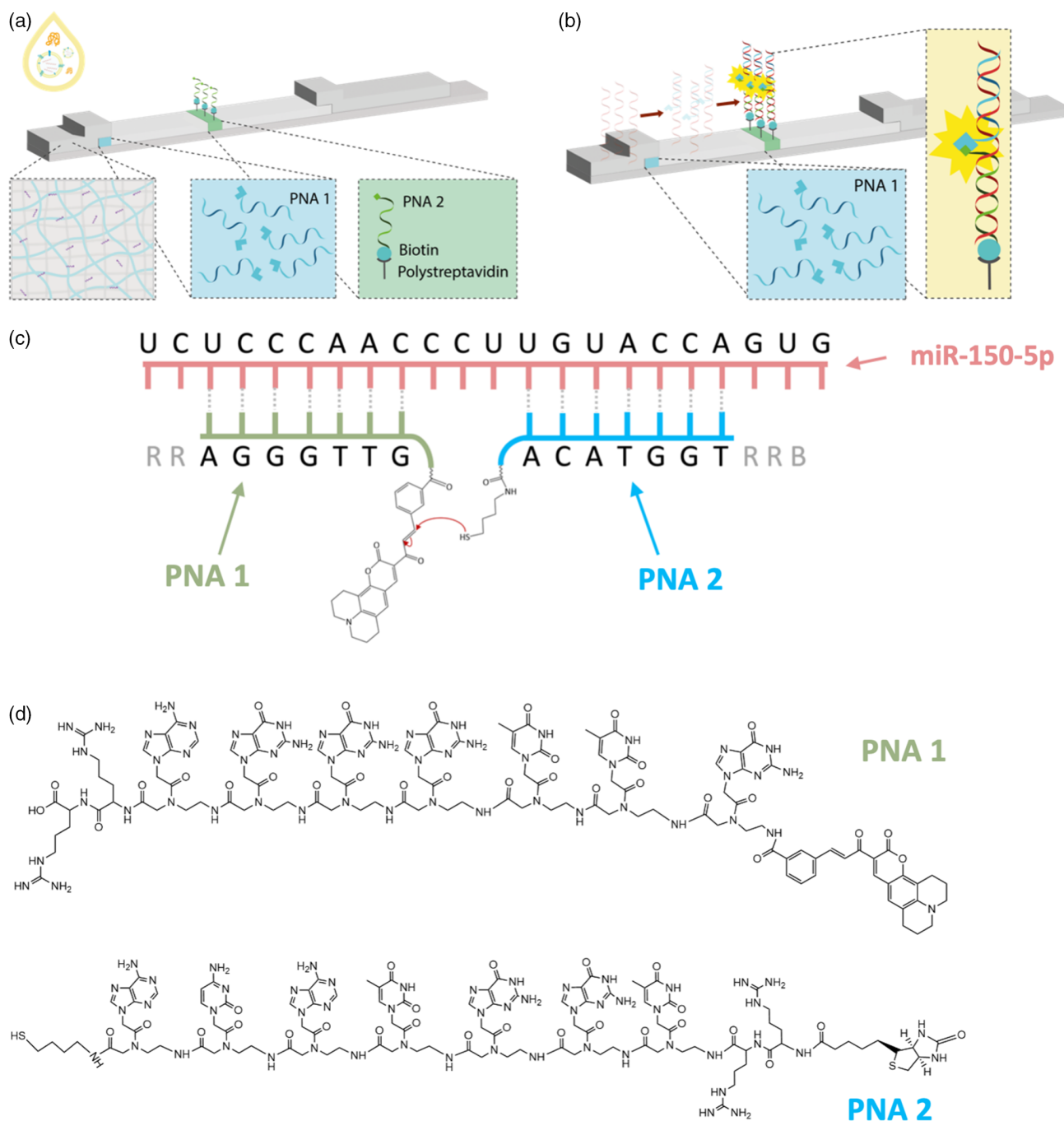


Figure 1. Schematic representation of the lateral flow test (LFT) for on-chip miR detection by oligonucleotide-templated reaction (OTR) directly from plasma a) before and b) after addition of plasma containing the target miR-150-5p. The endogenous miRs are released from their carriers using a denaturing hydrogel composite sample pad. After passing through the sample pad, they bind to peptide nucleic acid (PNA-1) which is printed on the nitrocellulose found under the sample pad. The hybridized complex formed between miR and PNA-1 then flows down the LFA and is captured by PNA-2 at the test line where the OTR takes place. c) miR-150-5p PNA probe design (R = Arginine, B = Biotin). d) Chemical structures of the bespoke PNA probes directed against miR-150-5p.

coumarin (PNA-1 used as a sensing probe) and a butane thiol (PNA-2 used as a capture probe) as previous reports (see Methods section). While the sensing probe was directly printed on the nitrocellulose underneath the sample loading pad, the capture probe (also containing a biotin moiety at its N-terminus) was

preincubated with polystreptavidin (pSA) in solution before printing and immobilization onto the nitrocellulose strip. This optimized manufacturing process offers significant advantages when compared to our initial design. First, it minimizes the requirement for off-chip sample manipulation such as

preincubation of the sample with the sensing probe prior to loading onto the LFT. This direct printing method of the PNA-pSA complex is also significantly more amenable to multiplexed analysis through simultaneous printing of multiple test lines, as envisaged for future applications. But most importantly, it also enables greater control of the amount of capture probe on the test line, enabling greater sensitivity, lower background noise, and a larger degree of tuneability for adjusting the sensor's dynamic range depending on the biomarker's natural abundance. An example of such improvement is shown in Figure S1, Supporting Information, with probes directed against miR-374a-5p, another miR upregulated in PTB, capable to detect target concentrations as low as 1 fM.

2.2. MiRNA Detection Directly from Plasma

Having significantly improved the performance of our LFT, the potential to detect miR-150-5p directly from blood plasma was investigated for the first time. This initial preclinical testing was performed using samples from patients who delivered at term ($n = 5$) and patients who either delivered preterm ($n = 2$) or had short cervix but were prevented from early delivery following cervical cerclage ($n = 3$). It is noteworthy that all samples were prospectively collected between 12th and 14th week of pregnancy, substantially earlier than any clinical symptom of PTB. Importantly, a signal above background noise was observed at

the test line for all 10 samples when loading as little as 3 μ L of plasma onto the strip with a statistically significant difference ($p = 0.0178$) between the two groups (term versus at risk of preterm), Figure 2a. This corresponded to an AUC of 0.69, Figure 2b.

2.3. Exploring the Role of Tween Surfactant

The potential role of Tween, commonly used as a surfactant in LFT running buffers to prevent nonspecific interactions and facilitate flow, was more specifically investigated using one clinical sample (Figure 2c). While removing Tween completely reduced the signal at the test line to near background level, a steady increase in signal was observed when increasing Tween concentration up to 2% with a plateau being reached at around 1% concentration. While this could be justified by the role played by Tween in regulating flow, it could also be explained by its ability to promote the breakdown of exosomes and the release of otherwise entrapped molecular biomarkers. This was tested in vitro using exosomes extracted from human plasma and dynamic light scattering (DLS), Figure 2d. Incubation of purified human exosomes with increasing Tween concentrations (0.5–2.0%) resulted in the reduced number and overall size of the microvesicles (Figure 2d) confirming the ability of low concentrations of Tween to breakdown exosomes.

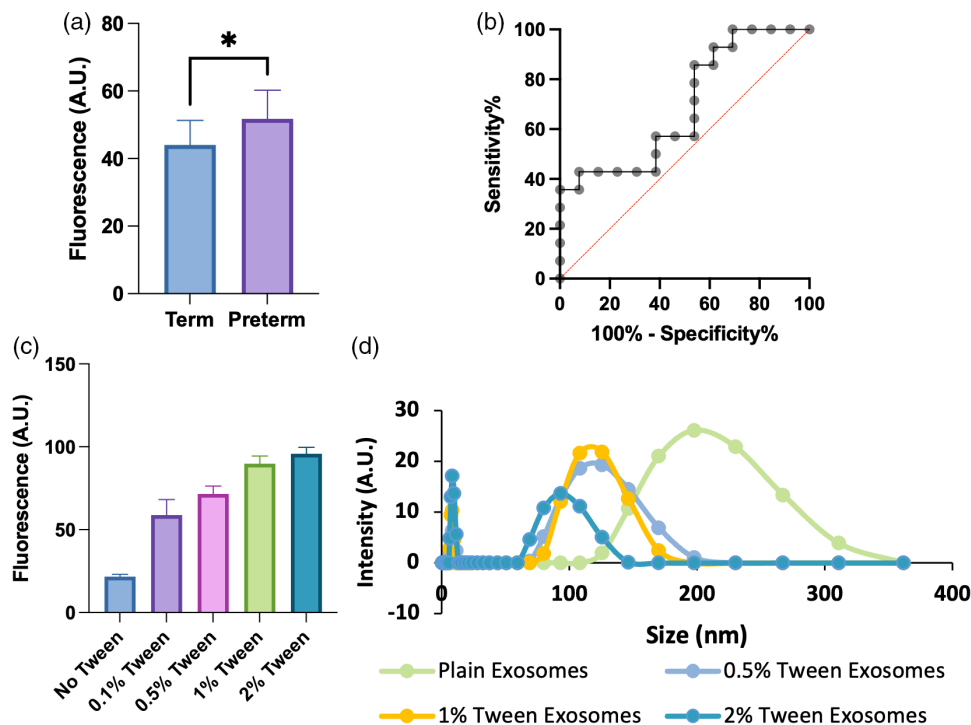


Figure 2. Detection of miR-150-5p directly from plasma on an LFA. a) Detection of miR-150-5p on the LFA with a plain cellulose sample pad, two-tailed student t test $p = 0.0178$ ($n = 5$ term, $n = 5$ PTB [preterm birth] or short cervix, 3 LFAs per clinical sample, 3 μ L of plasma onto each LFA, data are represented as mean \pm standard deviation); b) Receiver operator characteristic (ROC) curve with an area under the receiver operator characteristic curve (AUC) of 0.69; c) Effect of Tween on the size of the exosomes extracted from plasma, data are represented as mean \pm standard deviation; d) Comparison of the effect of different concentrations of Tween in the solution to which the plasma sample is added to dilute it before addition onto the LFA (3 μ L of one plasma sample added to all the LFAs after dilution in 25 μ L of 1X TBE and varying concentrations of Tween in this experiment, 3 LFAs used per Tween concentration).

2.4. Effect of Denaturing Sodium Dodecyl Sulfate Alginate Hydrogels of Protein and Exosome Integrity

Recent attempts have been reported that include hydrogels and LFT for pre-purification of samples prior to sensing. Here, we hypothesized that alginate hydrogels loaded with a powerful denaturing agent such as sodium dodecyl sulfate (SDS) could enhance the effects observed with Tween by simultaneously breaking down exosomes and unfolding proteins, thus releasing entrapped or complexed nucleic acid biomarkers from both carriers for downstream detection. The denaturing properties of SDS were first tested on bovine serum albumin (BSA, chosen here as a model protein) using either a fluorometric assay or circular dichroism (CD). SDS effects on the integrity of purified human exosomes were then examined by DLS. SDS-induced BSA unfolding in buffered solution was first observed in a fluorescence-based assays using 8-anilino-1-naphthalenesulfonic acid (ANS), a commonly used fluorophore to characterize protein binding sites^[35] in BSA. While ANS fluoresces upon binding to folded proteins, protein denaturation is commonly associated with a decrease in fluorescence. A maximum level of denaturation was observed at an SDS concentration of 2 mM close to its critical micellar concentration CMC (Figure 3b), a result further confirmed by CD experiments (Figures S2 and S3, Supporting Information). A similar trend was observed for the breakdown of exosomes monitored by DLS (Figure 3c). While

assessing protein and exosome integrities in hydrogel matrices is technically more challenging, BSA unfolding was investigated in SDS-loaded alginate hydrogels using the same ANS-based fluorometric assay and maximum denaturation was observed at a similar SDS concentration as previously observed in solution, demonstrating that SDS retains its denaturing properties when embedded with an alginate hydrogel (Figure S4, Supporting Information). Importantly for downstream applications, near-instantaneous denaturation was observed, consistent with previous reports.^[36]

2.5. Engineering, Characterization, and In Vitro Testing of a Cellulose–Hydrogel Composite Sample Pad

To further exploit the denaturing properties of SDS-loaded hydrogels for on-chip miR extraction from plasma and facilitate their incorporation into LFTs, we developed new cellulose–hydrogel composites by ionic (Ca²⁺-mediated) cross-linking of SDS-loaded sodium alginate impregnated into nitrocellulose pad. The new hybrid material microstructure was observed by scanning electron microscopy (SEM) revealing the coating of the cellulose fibers and confirming the presence of SDS molecules within the mesh structure, even after cross-linking and freeze-drying (Figure 4). Energy-dispersive X-ray spectroscopy (EDX) analysis allowed confirmation of the chemical nature of the structure (Figures S5 and S6, Supporting Information).

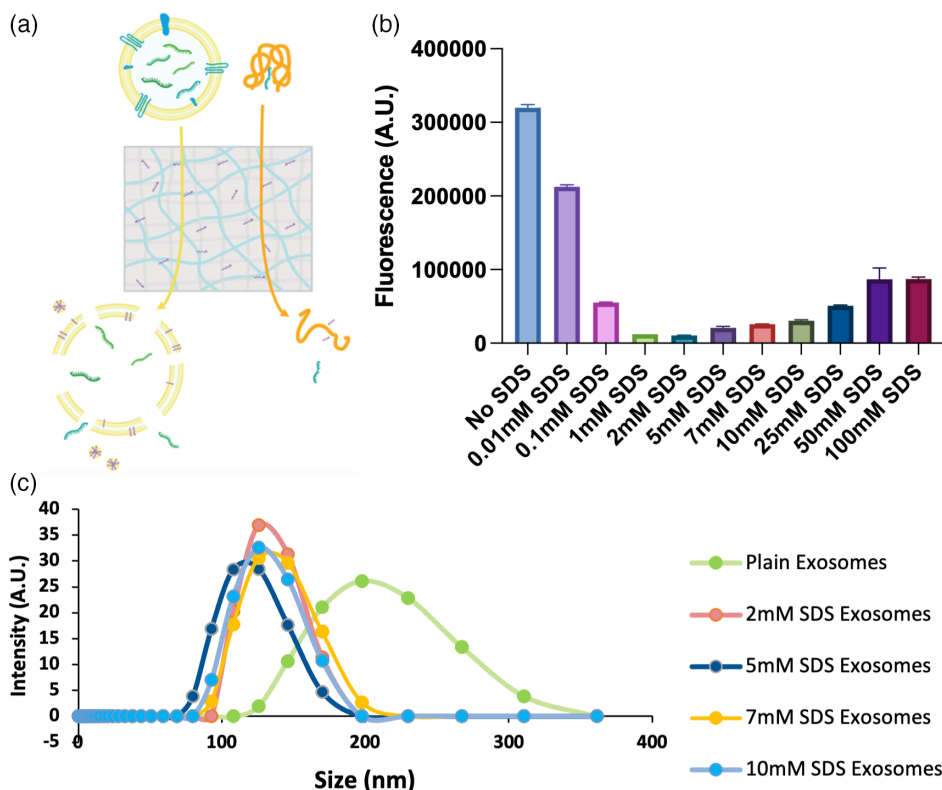


Figure 3. Effect of sodium dodecyl sulfate (SDS) on protein and exosome integrity. a) Schematic of miR release using denaturing hydrogel composite sample pads (grey mesh = cellulose, blue mesh = cross-linked alginate including added SDS); b) bovine serum albumin 8-anilino-1-naphthalenesulfonic (BSA-ANS) acid in solution scanned using a plate reader with three repeats per SDS concentration, data are represented as mean \pm standard deviation; c) size of exosomes with different SDS concentrations.

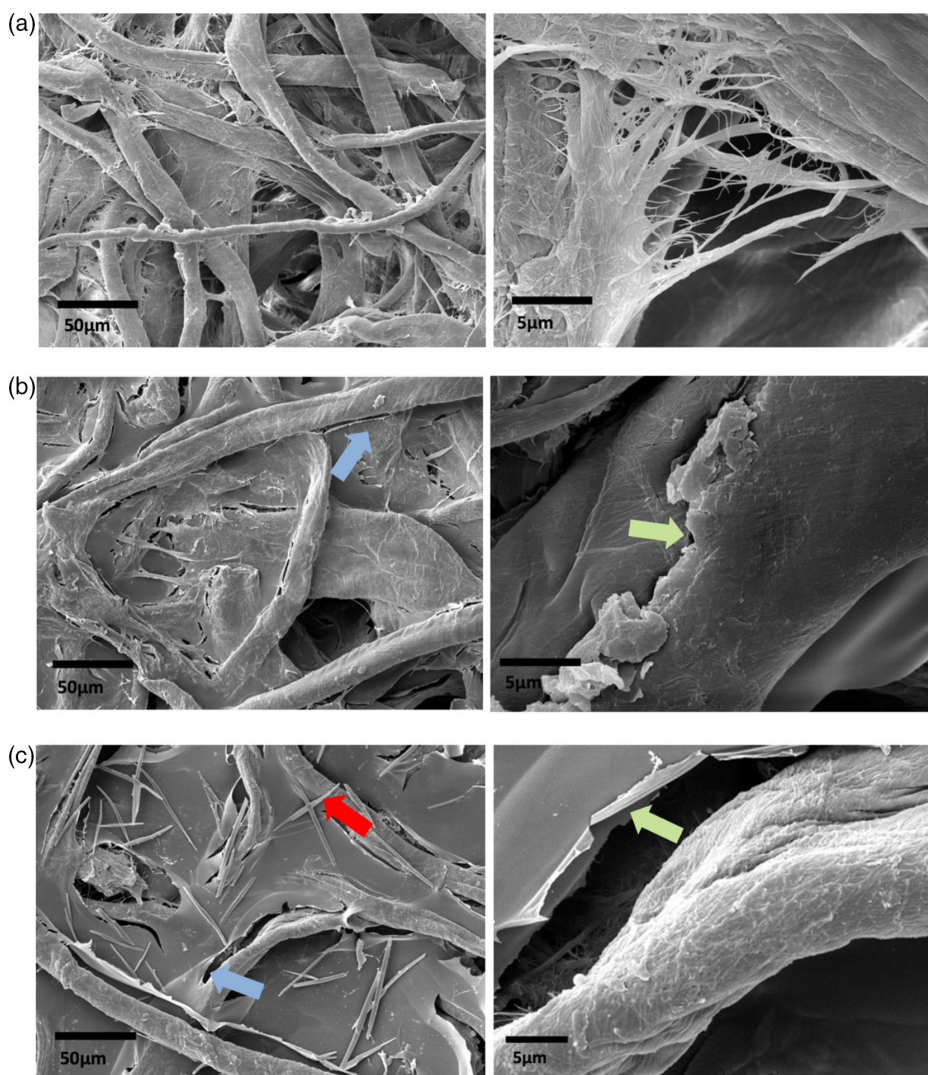


Figure 4. Scanning electron microscope (SEM) images of denaturing hydrogel–cellulose composite sample pads, scale bars represent 50 and 5 μm , respectively. a) SEM image of a cellulose sample pad without hydrogel; b) SEM image of a cellulose sample pad with a hydrogel incorporated showing the interweaving of the hydrogel between the cellulose fibers (blue and green arrows pointing at hydrogel); c) SEM image of a cellulose sample pad with a hydrogel incorporated showing the interweaving of the hydrogel between the cellulose fibers (blue and green arrows pointing at hydrogel) as well as SDS crystals (red arrow).

This new composite material was then used for the engineering of novel sample-loading pads that were cut to size ($0.5 \times 0.75 \text{ cm}$) and incorporated into our LFT in replacement of the traditional absorbent pads for preclinical testing.

2.6. Preclinical Validation of the Composite Sample Pads in LFTs

The potential use of this new composite material as a sample pad for LFTs was then assessed with one human plasma sample, while investigating the effect of SDS concentration (0, 5 and 10 mM) on signal intensity, **Figure 5a**. It was hypothesized that upon loading of the plasma sample onto the new pad, instantaneous denaturation of proteins and exosomes would increase the pool of endogenous miRs available for detection, while keeping larger molecules

and unfolded proteins trapped within the tight mesh structure. While comparably low signals were obtained when using a sample loading pad made of either pure cellulose or SDS-free cellulose–alginate hydrogel composite material, a significant increase in signal intensity was observed when SDS was included in the new hybrid material with a maximum effect observed at an SDS concentration of 10 mM. To further assess the benefits of the new denaturing hybrid material compared to the traditional sample pad, the same 10 clinical samples were tested on these new LFTs. A considerable increase in statistically significant difference ($p < 0.0001$) was observed when comparing the two groups (term delivery vs PTB or short cervix), with a new AUC of 0.97 (**Figure 5b,c**), comparable to that obtained by reverse-transcription quantitative polymerase chain reaction (RT-qPCR) for the same samples (**Figure S7**, Supporting Information).

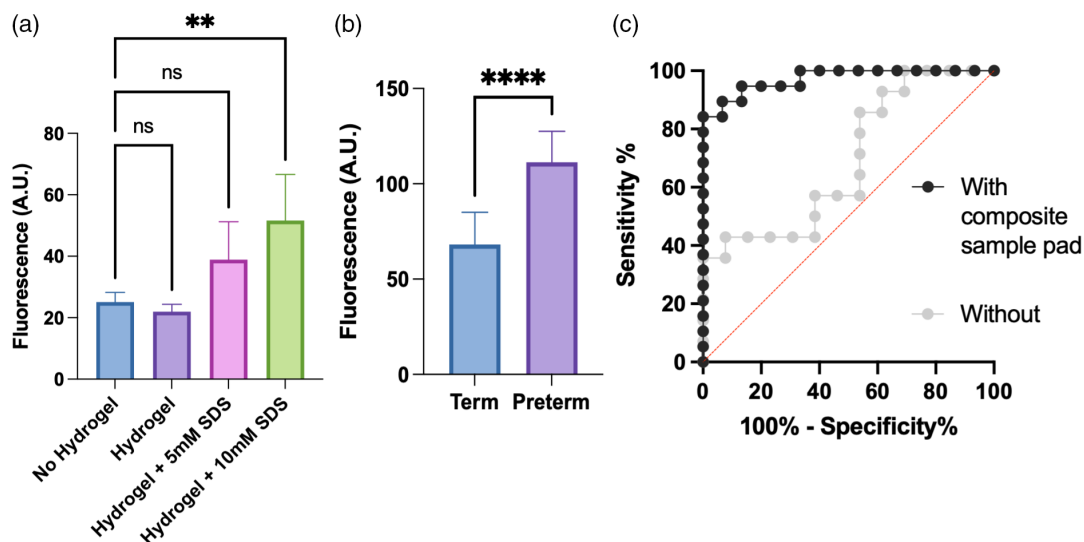


Figure 5. Denaturing hydrogel–cellulose composite sample pad for the detection of miR-150-5p from plasma. a) Effect of hydrogel–composite sample pads and different SDS concentrations incorporated in a hydrogel on the signal from the detection of miR-150-5p from a single clinical sample, 3 LFAs per different sample pad tested, one-way ANOVA with $p = 0.0041$ for 10 mM SDS content of sample pad; b) detection of miR-150-5p on the LFAs using the same 10 clinical samples as previously provided, two-tailed student t -test $p < 0.0001$ ($n = 5$ term, $n = 5$ PTB or short cervix, 3 LFAs per clinical sample, 3 μL of plasma onto each LFA); c) ROC curve with an AUC of 0.97. Data are represented as mean \pm standard deviation.

3. Discussion

In summary, we have demonstrated the optical detection of endogenous concentrations of miR-150-5p directly from 3 μL of human plasma on our next-generation LFT that required no target or signal amplifications nor any off-chip miR extraction prior to sensing. Our platform was able to distinguish between women at risk of preterm labor and those who were not with an AUC of 0.97, a degree of sensitivity and specificity comparable to that obtained with RT-qPCR analysis of miRs after extraction from maternal blood. Compared to other PTB tests currently available, our predictive LFT is not only capable of identifying women at high risk of PTB but also, and more importantly, is capable of predicting true outcome (i.e., actual preterm delivery and cervical shortening that without intervention can lead to PTB). Unlike other tests used in clinic, it is minimally invasive and does not rely on biomarkers that are only upregulated close to the time of labor (and therefore have a very limited predictive capacity) such as fetal fibronectin, placental alpha macroglobulin-1, or phosphorylated insulin-like growth factor binding protein-1, which are all detected from cervical secretions.^[37–40] This would allow the risk stratification to take place a lot earlier than with currently available screening tools and thus widen the window for outcome-modifying interventions. Although the excellent predictive value of miR150-5p as a stand-alone biomarker has already been demonstrated, current work is underway to develop a second-generation LFT that can detect at least two different miRs simultaneously, while also including a miR-independent control line.

The robustness and potential clinical utility of a diagnostic or predictive test is often compromised by the way biological specimens are collected and processed prior to analysis. Detection of low copy numbers of miRs for instance requires multiple enzyme-catalyzed amplification steps, which typically requires

target RNAs to be pre-purified and/or pre-concentrated. Such steps either i) require complex, multistep procedures and toxic chemicals unsuitable for incorporation into portable devices or ii) are inefficient and non-standardized therefore affecting the reliability/reproducibility of the test. Furthermore, the vast majority of commercially available processing kits are only suitable for one sample type and for a specific class of biomarkers (e.g., DNA vs RNA vs mRNA). Here, we have reported the successful use of a new generation of LFT sample pad for loading and automated (i.e., on-chip) processing of biological specimens prior to miR detection. It is based on a composite material made of cellulose and alginate hydrogel and incorporates a denaturing agent (SDS) for near instantaneous release of miR analytes from their carriers. Added upstream of the LFT-sensing region, where the specimen is usually deposited, this new pad can be easily substituted from more traditional sample loading pads and is likely to be compatible with a wide range of sensing technologies or readouts, well beyond the detection strategy used in our study.

4. Conclusion

Based on these findings, we anticipate that our versatile denaturing pads could help address one of the main issues faced by nucleic acid LFTs: their reliance on extensive and ineffective off-chip preprocessing and extraction steps. This has proven a major source of error and variability between studies/tests and has significantly slowed down the discovery and validation of miRNAs as clinically useful biomarkers. It also explains, at least in part, the current absence in the clinic of any POC diagnostic test based on miR detection. In its current simplex form, our technology could prove useful for the prediction or diagnosis of a broad range of conditions and pathologies for which single

deregulated miRs have proven clinically informative. An example of this is endometriosis screening, a debilitating condition affecting around 1 in 10 women where current diagnosis involves laparoscopic investigation. For this condition, a specific miR (miR-125-5p) was identified with a high predictive ability (AUC = 0.974).^[41]

5. Experimental Section

PNA Probe Design and Synthesis: Two 7-mer PNA probes were designed as previously reported by Metcalf et al. and Pavagada et al.^[27,28] that were complementary to two neighboring regions of miR-150-5p and separated by a three-nucleotide gap upon simultaneously hybridization to their target. PNA-1 was functionalized at its N-terminus by a quenched coumarin probe head while PNA-2 was dual-functionalized at its C-terminus and N-terminus by a butane thiol and biotin, respectively (Figure 1c). The probes were synthesized using manual solid phase peptide synthesis, characterized, and purified as described in the Supporting Information.

LFA Printing, Assembly, and Data Acquisition: PNA-2 (50 μM in water) containing the thiol and biotin moieties was first preincubated with pSA (0.01 mg mL^{-1} in water) for 60 min. The solution was then printed onto a nitrocellulose sheet (UniSart CN 95, Sartorius) at a rate of 0.2 mL min^{-1} using a ClaremontBio LFA printer (Automated Lateral Flow Reagent Dispenser), 16 mm from the top of the sheet. The mobile probe solution was prepared as a solution of PNA-coumarin (9.36 μM in 1X tris-Borate-EDTA (TBE) also containing 1% Tween-20) and printed at a rate of 0.35 mL min^{-1} , 1 mm from the top of the nitrocellulose sheet, which was then left to dry overnight. It was then placed onto a plastic acetate sheet using double-sided tape and finally the sample and absorbance pads (made from cellulose fiber sample pad, Merck) were placed to overlap with the nitrocellulose by 2.5 and 5 mm, respectively. The assembled LFA sheet was then cut into 5 mm wide strips, which were used as the final LFAs. All LFAs were stored in the dark at room temperature and used within two weeks of printing.

For clinical samples, 3 μL of plasma was added to 22 μL of a TBE/Tween-20 containing solution for a total concentration of 1X TBE and 1% Tween-20. This was then deposited onto the LFA, followed by another 25 μL of wash solution (1X TBE and 1% Tween-20) after 15 min. The LFAs were allowed to dry at room temperature for 30 min, after which they were actively dried for 2 min.

The LFAs were scanned using a bench-top fluorescence scanner (ESEQuant LR3, Qiagen) with an excitation wavelength of 470 nm and emission at 520 nm, at 5 points along the test line, and the peak fluorescence integrals were averaged for each LFA. Each clinical sample was tested on three separate LFAs.

Denaturing Sample Pad Preparation: For on-chip sample processing, cellulose sample pads were cut to size (0.5 \times 0.75 cm) and impregnated with 40 μL of 3% alginate with or without SDS. The concentration of alginate was chosen to achieve a predicted pore size of \approx 16–18 nm which was small enough for miRNA diffusion while restricting the diffusion of larger biomolecules.^[42] After 5 min, to allow the hydrogel to spread homogeneously, the sample pads were placed into 100 mM calcium chloride solutions for 12 min to allow cross-linking of the alginate. Upon removal, the modified pads were frozen at -80°C overnight followed by lyophilization over 48 h.

Plasma Preparation: Ethical approval was granted by the Hertfordshire Research Ethic Committee (22/02/2011-REC reference number 11/H0311/6). Whole blood was obtained from patients who attended clinics at Imperial College Healthcare NHS Trust (London, UK), following informed, written consent at 12–14⁺ weeks of gestation. Women with multiple pregnancies, with preexisting diseases, and those who subsequently developed other obstetric complications including preeclampsia, gestational hypertension, gestational cholestasis, and obstetric cholestasis were excluded from the study.

The procedure was conducted in accordance with all relevant guidelines and regulations. Blood samples were immediately placed on ice before

centrifugation at 1300 \times g for 10 min at 4 $^\circ\text{C}$ within 30 min of collection to isolate plasma. Plasma samples were aliquoted and stored in RNase-free microtubes at -80°C .

RNA Extraction and RT-qPCR: Plasma aliquots were thawed on ice prior to centrifugation at 800 \times g for 10 min at 4 $^\circ\text{C}$, and only the upper 750 μL of plasma was used for the RNA extraction to avoid cellular and/or platelet contamination.^[43] RNAs were obtained with the Plasma/Serum Circulating and Exosomal RNA Purification Mini Kit (Slurry Format) (Norgen Biotek, Ontario, Canada) as previously reported by Kim et al.^[44] Reverse transcription of extracted plasma RNA was performed using miRCURY LNATM Universal RT miRNA cDNA synthesis kit II (Exiqon, Vedbaek, Denmark) with the addition of UniSp6 (108 copies mL^{-1}) to allow normalization of variation that may occur during the reverse-transcription process, while the LinRegPCR program v2017.1^[45] was used to determine Cq values and primer efficiency for all samples and miRNA targets, as previously reported by Kim et al.^[44]

Exosome Preparation and Size Distribution: Exosomes were extracted from 500 μL of plasma using size-exclusion chromatography (SEC) columns (qEVoriginal/70 nm, IZON) in the Automatic Fraction Collector (IZON) according to manufacturer's instructions, using phosphate-buffered saline (PBS) as calibration buffer. The void volume was 3 mL, followed by 500 μL fractions. Nanoparticle tracking analysis (NTA) was performed to measure the concentration and size of the exosomes using the ZetaView 8.05.12 SP2 software (Particle Metrix). The exosome containing fractions 1–3 were diluted in 1 mL PBS to get the recommended concentration measurement range of 50–200 particles/frame. The instrument measured 11 positions for each fraction, with duplicate readings per position. The instrument parameters were 23 $^\circ\text{C}$, sensitivity at 75, frame rate of 30 frames s^{-1} , shutter speed of 100, and laser pulse duration equal to shutter duration. Instrument calibration was performed using polymer beads (Cat. No. 3100A, ThermoFisher) prior to NTA.

Monitoring Protein Denaturation with ANS Acid: In a typical experiment, 40 μM BSA and 4 μM ANS in 1X PBS were used following the methodology of Togashi et al.^[45,46] and the fluorescence was detected using a CLARIOstar Plus plate reader (BMG Labtech), using an excitation wavelength of 380 nm and emission of 470 nm.

Circular Dichroism: CD spectra of a solution of BSA (1 mL), 1 μM in 1X PBS in the presence and absence of SDS, were recorded on a Chirascan V100 instrument (AppliedPhotophysics) using the following scanning parameters of 0.5 s per point, 10 mm pathlength, 1 nm step size, and scanning window between 200 and 280 nm.

Statistical Analysis: The averages within each group were tested for normality using the Shapiro–Wilk test and for comparison between two groups, a two-tailed student *t*-test was used. For data comparing multiple groups, a one-way analysis of variance (ANOVA) test was used followed by a Dunnett's post hoc test. $P < 0.05$ was considered statistically significant and data were graphically represented as mean \pm standard deviation and statistical analysis was conducted on GraphPad Prism (Version 9.2.0).

Supporting Information

Supporting Information is available from the Wiley Online Library or from the author.

Acknowledgements

The authors thank the March of Dimes for financial support. This work was also supported by the National Institute of Health Research (NIHR) Imperial Biomedical Research Centre (BRC) and LS was supported by the NIHR Clinical Lectureship Scheme and is a Parasol Foundation Clinical Senior Lecturer in Obstetrics.

Conflict of Interest

The authors declare no conflict of interest.

Data Availability Statement

The data that support the findings of this study are available on request from the corresponding author. The data are not publicly available due to privacy or ethical restrictions.

Keywords

denaturing hydrogels, lateral flow tests, liquid biopsies, microRNAs, predictive biomarkers, preterm birth

Received: March 11, 2022

Revised: April 11, 2022

Published online: June 16, 2022

-
- [1] L. Liu, S. Oza, D. Hogan, J. Perin, I. Rudan, J. E. Lawn, S. Cousens, C. Mathers, R. E. Black, *Lancet* **2015**, 385, 430.
- [2] J. E. Lawn, M. Kinney, *Sci. Transl. Med.* **2014**, 6, 263ed221.
- [3] S. Saigal, L. W. Doyle, *Lancet* **2008**, 371, 261.
- [4] A. T. Bhutta, M. A. Cleves, P. H. Casey, M. M. Cradock, K. J. S. Anand, *JAMA* **2002**, 288, 728.
- [5] D. Moster, R. T. Lie, T. Markestad, *N. Engl. J. Med.* **2008**, 359, 262.
- [6] M. Son, E. S. Miller, *Semin. Perinatol.* **2017**, 41, 445.
- [7] J. D. Iams, *N. Engl. J. Med.* **2014**, 370, 254.
- [8] J. Höck, G. Meister, *Genome Biol.* **2008**, 9, 210.
- [9] R. W. Carthew, E. J. Sontheimer, *Cell* **2009**, 136, 642.
- [10] T. P. Chendrimada, K. J. Finn, X. Ji, D. Baillat, R. I. Gregory, S. A. Liebhaber, A. E. Pasquinelli, R. Shiekhattar, *Nature* **2007**, 447, 823.
- [11] S. Deng, G. A. Calin, C. M. Croce, G. Coukos, L. Zhang, *Cell Cycle* **2008**, 7, 2643.
- [12] R. Garzon, M. Fabbri, A. Cimmino, G. A. Calin, C. M. Croce, *Trends Mol. Med.* **2006**, 12, 580.
- [13] M. D. Jansson, A. H. Lund, *Mol. Oncol.* **2012**, 6, 590.
- [14] J. Cook, P. R. Bennett, S. H. Kim, T. G. Teoh, L. Sykes, L. M. Kindinger, A. Garrett, R. Binkhamis, D. A. MacIntyre, V. Terzidou, *Sci. Rep.* **2019**, 9, 5861.
- [15] Y. Gu, J. Sun, L. J. Groome, Y. Wang, *Am. J. Physiol. Endocrinol. Metab.* **2013**, 304, E836.
- [16] S. Khanjani, M. K. Kandola, T. M. Lindstrom, S. R. Sooranna, M. Melchionda, Y. S. Lee, V. Terzidou, M. R. Johnson, P. R. Bennett, *J. Cell. Mol. Med.* **2011**, 15, 809.
- [17] N. Wang, Z. Zhou, T. Wu, W. Liu, P. Yin, C. Pan, X. Yu, *Open Biol.* **2016**, 6, 150258.
- [18] L. Xu, B. F. Yang, J. Ai, *J. Cell. Phys.* **2013**, 228, 1713.
- [19] P. S. Mitchell, R. K. Parkin, E. M. Kroh, B. R. Fritz, S. K. Wyman, E. L. Pogosova-Agadjanyan, A. Peterson, J. Noteboom, K. C. O'Briant, A. Allen, D. W. Lin, N. Urban, C. W. Drescher, B. S. Knudsen, D. L. Stirewalt, R. Gentleman, R. L. Vessella, P. S. Nelson, D. B. Martin, M. Tewari, *Proc. Natl. Acad. Sci. U. S. A.* **2008**, 105, 10513.
- [20] J. Guduric-Fuchs, A. O'Connor, B. Camp, C. L. O'Neill, R. J. Medina, D. A. Simpson, *BMC Genomics* **2012**, 13, 357.
- [21] M. L. Squadrito, C. Baer, F. Burdet, C. Maderna, G. D. Gilfillan, R. Lyle, M. Ibberson, M. De Palma, *Cell Rep.* **2014**, 8, 1432.
- [22] J. D. Arroyo, J. R. Chevillet, E. M. Kroh, I. K. Ruf, C. C. Pritchard, D. F. Gibson, P. S. Mitchell, C. F. Bennett, E. L. Pogosova-Agadjanyan, D. L. Stirewalt, J. F. Tait, M. Tewari, *Proc. Natl. Acad. Sci. U. S. A.* **2011**, 108, 5003.
- [23] A. Turchinovich, L. Weiz, A. Langheinz, B. Burwinkel, *Nucleic Acids Res.* **2011**, 39, 7223.
- [24] A. Gallo, M. Tandon, I. Alevizos, G. G. Illei, *PLoS One* **2012**, 7, 30679.
- [25] L. Petrou, S. Ladame, *Lab Chip* **2022**, 22, 463.
- [26] S. Cai, T. Pataillot-Meakin, A. Shibakawa, R. Ren, C. L. Bevan, S. Ladame, A. P. Ivanov, J. B. Edel, *Nat. Commun.* **2021**, 12, 3515.
- [27] G. A. D. Metcalf, A. Shibakawa, H. Patel, A. Sita-Lumsden, A. Zivi, N. Rama, C. L. Bevan, S. Ladame, *Anal. Chem.* **2016**, 88, 8091.
- [28] S. Pavagada, R. B. Channon, J. Y. H. Chang, S. H. Kim, D. MacIntyre, P. R. Bennett, V. Terzidou, S. Ladame, *Chem. Commun.* **2019**, 55, 12451.
- [29] M. Sajid, A.-N. Kawde, M. Daud, *J. Saudi Chem. Soc.* **2015**, 19, 689.
- [30] J. Sayers, R. J. Payne, N. Winssinger, *Chem. Sci.* **2018**, 9, 896.
- [31] L. Farrera-Soler, A. Gonse, K. T. Kim, S. Barluenga, N. Winssinger, *Biopolymers* **2022**, 23485.
- [32] R. A. M. Brown, M. R. Epis, J. L. Horsham, T. D. Kabir, K. L. Richardson, P. J. Leedman, *BMC Biotechnol.* **2018**, 18, 16.
- [33] A. Brunet-Vega, C. Pericay, M. E. Quílez, M. J. Ramírez-Lázaro, X. Calvet, S. Lario, *Anal. Biochem.* **2015**, 488, 28.
- [34] A. Podolska, B. Kaczowski, T. Litman, M. Fredholm, S. Cirera, *Acta Biochim. Pol.* **2011**, 58.
- [35] O. K. Gasyimov, B. J. Glasgow, *Biochim. Biophys. Acta* **2007**, 1774, 403.
- [36] D. Winogradoff, S. John, A. Aksimentiev, *Nanoscale* **2020**, 12, 5422.
- [37] H. Khambay, L. A. Bolt, M. Chandiramani, A. De Greeff, J. E. Filmer, A. H. Shennan, *J. Obstetrics Gynaecol.* **2012**, 32, 132.
- [38] R. Pirjani, A. Moini, A. Almasi-Hashiani, M. F. Mojtahedi, S. Vesali, L. Hosseini, M. Sepidarkish, *J. Maternal Fetal Neonatal Med.* **2021**, 34, 3445.
- [39] H. Leitich, A. Kaidler, *BJOG* **2003**, 110, 66.
- [40] H. Honest, L. M. Bachmann, J. K. Gupta, J. Kleijnen, K. S. Khan, *BMJ* **2002**, 325, 301.
- [41] E. Cosar, R. Mamillapalli, G. S. Ersoy, S. Cho, B. Seifer, H. S. Taylor, *Fertil. Steril.* **2016**, 106, 402.
- [42] J. Klein, J. Stock, K.-D. Vorlop, *Eur. J. App. Microbiol. Biotech.* **1983**, 18, 86.
- [43] H. H. Cheng, H. S. Yi, Y. Kim, E. M. Kroh, J. W. Chien, K. D. Eaton, M. T. Goodman, J. F. Tait, M. Tewari, C. C. Pritchard, *PLoS One* **2013**, 8, e64795.
- [44] S. H. Kim, D. A. MacIntyre, R. Binkhamis, J. Cook, L. Sykes, P. R. Bennett, V. Terzidou, *EBioMedicine* **2020**, 62, 103145.
- [45] J. Ruijter, C. Ramakers, W. M. H. Hoogaars, Y. Karlen, O. Bakker, M. J. B. van den Hoff, A. F. M. Moorman, *Nucleic Acids Res.* **2009**, 37, 45.
- [46] D. M. Togashi, A. G. Ryder, D. O'Shaughnessy, *J. Fluoresc.* **2010**, 20, 441.